for a fixed value $|z| = 1000$. This rotation causes z to approach the Stokes lines, which are near $\theta = 1^o$. It is seen that for all orders the relative errors are maximum near this region. In Fig. 2, comparisons between truncation 1 and exact results are shown. The Wronskian computations were done for $m = 0$, corresponding to $\eta = 0$. The results clearly indicate that the truncation is subject to errors.

For commonly used practical microstrip configurations, the relation

$$L = k_0 d\sqrt{\epsilon_r - 1} \leq \frac{\pi}{2} \tag{14}$$

is well known [2]. Here d is the substrate thickness, ϵ_r is the relative permittivity, and L is the electrical length. This will excite one TM surface- and one TE leaky-wave pole [1]. For $\epsilon_r = 4$, we find from [9, Fig. 4] that $\beta_p/k_0 \simeq 2.7 - j8.0$. Substituting these values in (1) we get

$$z \simeq 53.35\frac{\rho}{\lambda}e^{+j1.89}. \tag{15}$$

As shown in [2, Figs. 1, 2, 5, 6], lateral separations of $\rho \geq 20\lambda$ are not uncommon in designing large arrays. Setting $\rho = 20\lambda$ in (18) gives $|z| \simeq 1067$. One can conclude from Figs. 1 and 2 that truncations in the asymptotic series for $H_0^{(2)}(z)$, for $|z| \geq 1000$, can be subject to increased numerical errors.

Our results indicate that the Stokes phenomenon could eventually dictate the accuracy of computing the mutual coupling for medium or large microstrip arrays. Techniques such as the Borel summation formula [8, pp. 405–408] appear applicable although much work remains to be done in the future.

IV. Summary

In this paper we have studied the effects of truncations of the infinite asymptotic series for the Hankel function that appears in the Sommerfeld integral for the microstrip Green's function. For large values of the complex argument z, such truncated expansions can be inaccurate. This inaccuracy is a manifestation of the Stokes phenomenon that depends both on the magnitude and phase of the complex argument z, which depends on the substrate geometry and the lateral separation between antennas. When z tends to a transition (or distinguished) point z_0, certain rays in the complex z plane are crossed, across which the truncated asymptotic expansion is no longer analytically continuable; these are called Stokes lines. This leads to numerical inaccuracies that may manifest themselves in calculating mutual coupling between widely separated elements in a microstrip array. It has been found numerically that for $|z| \geq 1000$ the Stokes phenomenon manifests itself when the Green's function is computed; hence, the mutual coupling between microstrip antennas. This value generally corresponds to the dimensions of a medium-sized array for electrically thin substrates with relatively low permittivities. To rectify the Stokes phenomenon the Borel summation formula may be used, but its application to the asymptotic evaluation of the Sommerfeld integral remains a challenging topic for future research.

References

[1] S. Barkeshli, P. H. Pathak, and M. Marin, "An asymptotic closed-form microstrip surface Green's function for the efficient moment method analysis of mutual coupling in microstrip antennas," *IEEE Trans. Antennas Propagat.*, vol. 38, no. 9, pp. 1374–1383, Sept. 1990.

[2] P. R. Haddad and D. M. Pozar, "Anomalous mutual coupling between microstrip antennas," *IEEE Trans. Antennas Propagat.*, vol. 42, no. 11, pp. 1545–1549, Nov. 1994.

[3] C. F. du Toit, "The numerical computation of Bessel functions of first and second kind for integer orders and complex arguments," *IEEE Trans. Antennas Propagat.*, vol. 38, no. 9, pp. 1341–1349, Sept. 1990.

[4] L. B. Felsen and N. Marcuvitz, *Radiation and Scattering of Waves*. Piscataway, NJ: IEEE Press, 1994.

[5] M. Abramowitz and I. A. Stegun, *Handbook of Mathematical Functions and Tables*. New York: Dover, 1970.

[6] N. Bleistien and R. A. Handelsman, *Asymptotic Expansion of Integrals* New York: Dover, 1986.

[7] F. W. J. Olver, *Asymptotics and Special Functions*. New York: Academic, 1974.

[8] R. B. Dingle, *Asymptotic Expansions: Their Derivation and Interpretation*. New York: Academic, 1973.

[9] C.-I. G. Hsu, R. F. Harrington, J. R. Mautz, and T. K. Sarkar, "On the location of leaky wave poles for a grounded dielectric slab," *IEEE Trans. Microwave Theory Tech.*, vol. 39, no. 2, pp. 346–349, Feb. 1991.

[10] D. Chatterjee and R. G. Plumb, "A hybrid formulation for the probe-to-patch attachment mode current for rectangular microstrip antennas," *IEEE Trans. Antennas Propagat.*, vol. 44, no. 5, pp. 677–687, May 1996.

A Fast Algorithm for Computing Field Radiated by an Insulated Dipole Antenna in Dissipative Medium

Lin-Kun Wu, David Wen-Feng Su, and Bin-Chyi Tseng

Abstract—**A fast algorithm for determining the near-field characteristics of an insulated dipole antenna (IDA) embedded in a homogenous dissipative medium is described in this paper. A thin-wire-approximation type of analysis is followed here. In this case, radiation is considered to originate from a filamentary current flowing along the axis of the dipole, which is surrounded immediately by the ambient dissipative medium. The translational symmetry inherent in the resultant radiation integrals is then exploited to speed up the computation. In one case studied, the basic thin-wire approach that uses no symmetry property is found to yield accurate results in approximately 380 times less CPU time than the traditional King–Casey approach. In another case, use of symmetry property further reduces the CPU time by a factor of 7; additional reduction in CPU time is possible by taking into account the near-field nature of the problem.**

I. Introduction

Analysis of the near field characteristics of an insulated dipole antenna (IDA) is fundamental in the design and evaluation of the heating performance of an interstitial microwave hyperthermia system. For the field computation purpose, IDA's may be classified as being either uniformly or nonuniformly insulated. In this paper, a fast computing algorithm will be developed explicitly for the uniformly insulated IDA's shown in Fig. 1, and extension to the nonuniformly insulated IDA's will also be described.

Two types of analysis have been employed in the past. In the King-Casey analysis of the symmetrically fed, uniformly insulated IDA shown in Fig. 1(a) [1], [2], the IDA is first treated as a lossy transmission line while determining the antenna input impedance and equivalent electric and magnetic current sources present over the exterior surface of the insulating catheter. The latter are then used

Manuscript received November 11, 1995; revised August 26, 1996. This work was supported by the National Science Council of the Republic of China under Grants NSC 83-0420-E-009-002 and NSC 84-2213-E-009-052.

The authors are with the Institute of Communication Engineering, National Chiao Tung University, Hsinchu 30039, Taiwan.

Publisher Item Identifier S 0018-9480(96)08490-6.

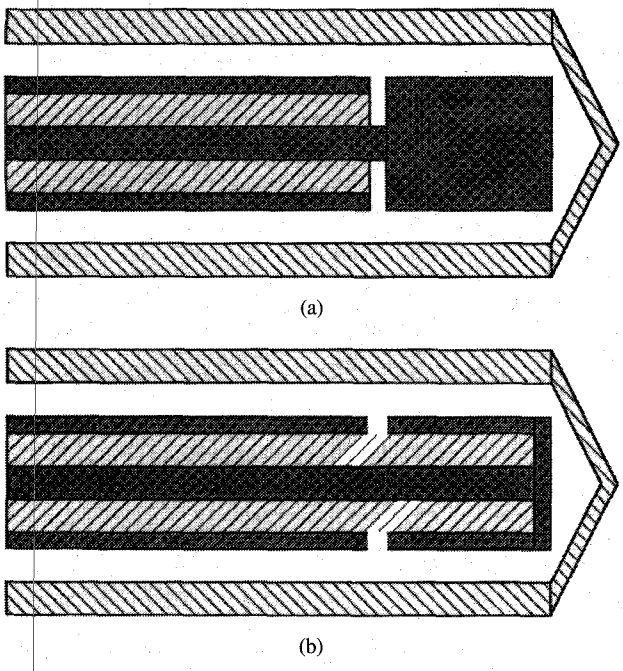

Fig. 1. Uniformly insulated dipole antennas used by (a) King *et al.* [1] and Casey and Bansal [2] and (b) Zhang *et al.* [4], [5].

to compute the field radiated by the dipole. Extensions to IDA's having three insulating layers and asymmetrical feeding arrangement can be found in [3] and [4], respectively. In these cases, the radiation integrals are double integrals with very complicated integrands and, therefore, are computationally demanding [5], [6].

An alternative method was developed and used by Iskander and Tumeh to analyze the performance of multisectioned IDA's [7]. In this method, dipole is replaced by an equivalent filamentary current flowing along the axis of the dipole and completely surrounded by the dissipative ambient medium. As such, one-dimensional (1-D) radiation integrals with much simpler integrands are obtained. This approach is obviously computationally more efficient than the traditional King-Casey approach. As will be shown in Section II, with a careful arrangement of the expressions associated with the resulting radiation integrals, their inherent translational symmetry can be identified and exploited to speed up the computation. Accuracy and computational efficiency of the resultant algorithm will be presented in Section III.

II. Formulation

Considering the problem geometry shown in Fig. 2 the actual source of radiation is the current on the surface of the dipole conductor of radius a, which is the same as the outer radius of the outer conductor of the coaxial cable used to construct and feed the IDA's. The antenna junction is located at where the outer conductor of the coaxial feedline is truncated for the IDA of Fig. 1(a) and at the circumferential slot formed over the outer conductor of the short-circuited coaxial feedline for the IDA of Fig. 1(b). In general, we consider the IDA to be asymmetrically driven [4], i.e., $h_1 \neq h_2$. The space between the dipole and catheter is assumed to be filled with air such that $\varepsilon_2 \approx \varepsilon_o = 8.854 \times 10^{-12}$ F/m. The catheter is assumed to be lossless with a real permittivity ε_3. The ambient dissipative medium is nonmagnetic and has a complex permittivity ε_4. Time dependence of $e^{j\omega t}$ is assumed and suppressed.

According to Iskander and Tumeh's thin-wire approximations [7], an equivalent field-radiating filamentary current source is assumed to

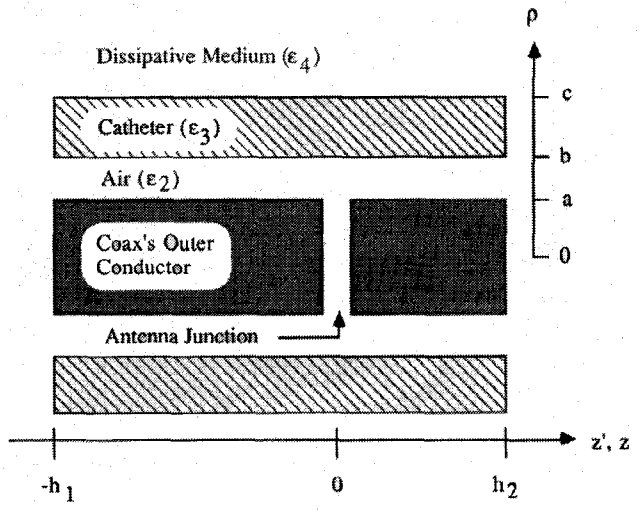

Fig. 2. Structural geometry of the uniformly insulated dipole.

flow along the axis of the dipole and surrounded immediately by the dissipative ambient medium. For the uniformly insulated IDA's, the resulting current distribution can be written as [4]

$$I(z') = I_0 \frac{\sin k_L(h_i - |z'|)}{\sin k_L h_i} \tag{1}$$

where $-h_1 \leq z' \leq 0$ for $i = 1$ and $0 \leq z' \leq h_2$ for $i = 2$. In (1), the current at the antenna junction I_0 and complex wavenumber k_L are defined in [1].

Referring to the geometry shown in Fig. 3, the spherical electric field components, dE_R and dE_θ, radiated from the current filament $I(z')\,dz'$ are obtained first [8], from which the spherical components of the total electric field radiated can be found as

$$E_R = \int_{-h_1}^{h_2} dE_R = \int_{-h_1}^{h_2} I(z')(F_R \cos\theta'' - F_\theta \sin\theta'')\,dz' \tag{2}$$

$$E_\theta = \int_{-h_1}^{h_2} dE_\theta = \int_{-h_1}^{h_2} I(z')(F_R \sin\theta'' + F_\theta \cos\theta'')\,dz' \tag{3}$$

where $\theta'' = \theta' - \theta$ and with $\eta_4 = (\mu_o/\varepsilon_4)^{1/2}$ and $k_4 = j\omega(\mu_o\varepsilon_4)^{1/2}$ being, respectively, the complex intrinsic impedance and wavenumber of the ambient medium

$$F_R = \frac{e^{-jk_4R'}}{2\pi}\left(\frac{\eta_4}{R'^2} + \frac{1}{j\omega\varepsilon_4 R'^3}\right)\frac{z - z'}{R'} \tag{4}$$

$$F_\theta = \frac{e^{-jk_4R'}}{4\pi}\left(\frac{j\omega\mu_0}{R'} + \frac{\eta_4}{R'^2} + \frac{1}{j\omega\varepsilon_4 R'^3}\right)\frac{\rho}{R'} \tag{5}$$

$$R' = \sqrt{\rho^2 + (z - z')^2}. \tag{6}$$

The corresponding cylindrical field components can be found from

$$E_\rho = E_R \sin\theta + E_\theta \cos\theta \tag{7}$$

$$E_z = E_R \cos\theta - E_\theta \sin\theta. \tag{8}$$

For observers located along a longitudinal line with fixed $\rho = \rho_o$, an examination of (4)–(6) reveals the following translational symmetry properties associated with F_R and F_θ

$$F_R = F_R(\rho_o, z; z') = \begin{cases} F_R(\rho_o, |z - z'|) & \text{if } z \leq z' \\ -F_R(\rho_o, |z - z'|) & \text{if } z \geq z' \end{cases} \tag{9}$$

$$F_\theta = F_\theta(\rho_o, z; z') = F_\theta(\rho_o, |z - z'|) \quad \text{for all } z \text{ and } z'. \tag{10}$$

Exploitation of this property to speed up the field computation process is described next.

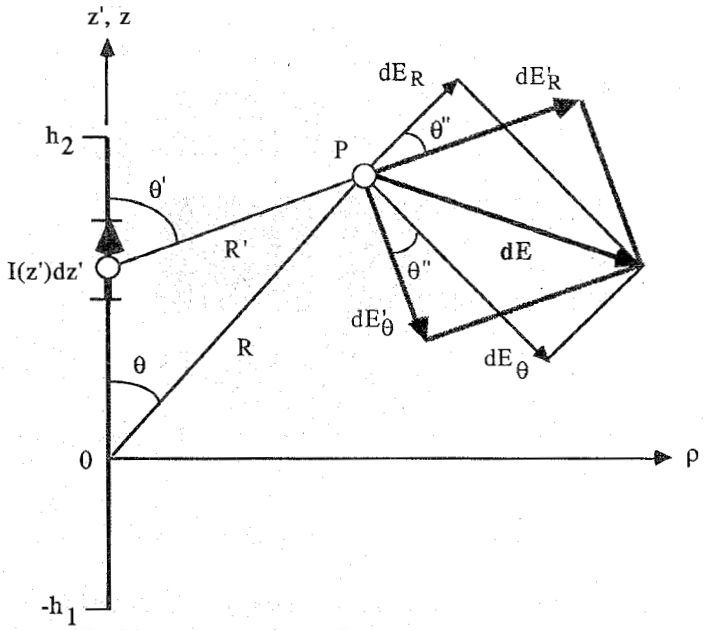

Fig. 3. Radiation from a filamentary current source model of the IDA.

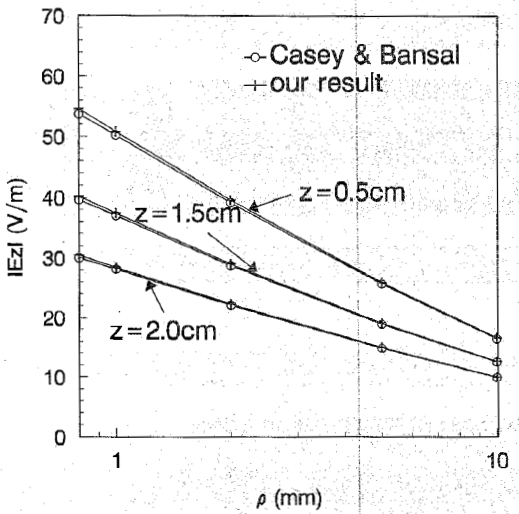

Fig. 4. Radial variations of $|E_z|$ computed by Casey and Bansal [2] and the present method without using the symmetry property at three different values of z.

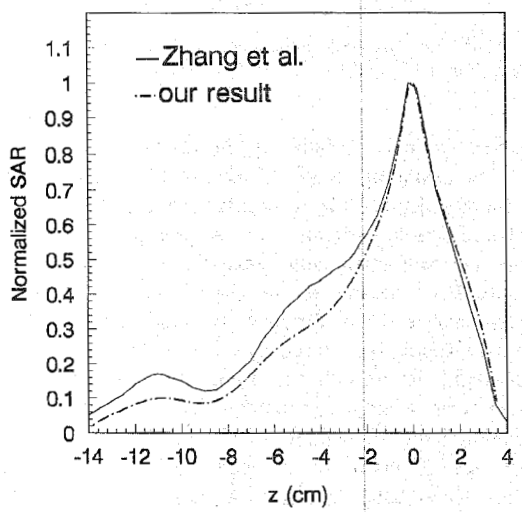

Fig. 5. Comparison of the normalized SAR obtained by Zhang *et al.* [4] and the present method using the symmetry property for observers located along the $\rho = 5$ mm longitudinal line.

Considering that the filamentary current source is divided into M segments of equal length $\Delta z'$ and fields at N discrete locations of constant spacing Δz are to be determined along a given longitudinal line. By requiring Δz to be an integral multiple of $\Delta z'$ and the first (or, in fact, any one of the N) observer(s) to have the same z-coordinate as that of the center of the first (or, any) source segment, the z coordinates of any source-observer pair will be differed by an integral multiple of $\Delta z'$, i.e., for $n = 1, 2, \cdots, N$ and $m = 1, 2, \cdots M$

$$|z_n - z'_m| = K\Delta z', \qquad K = 0, 1, 2, \cdots, K_{\max} \qquad (11)$$

where $K_{\max}$ is determined by the ratio between Δz and $\Delta z'$ and the maximum source-observer separation of interest. Given these, one needs only to compute and store a set of $K_{\max} + 1 F_R$'s and F_θ's and recall them for repetitive use when evaluating the discrete form of (2) and (3) for each of the N observers located along the given longitudinal line.

III. Results

To validate the thin-wire approximations used in the present method, the fields associated with a symmetrically-driven half-wave IDA previously analyzed by Casey and Bansal [2] are examined first. In this case, $f = 915$ MHz, $a = 0.47$ mm, $b = 0.584$ mm, $c = 0.8$ mm, $h_1 = h_2 = 3.1$ cm, $\varepsilon_2 \approx \varepsilon_o$, $\varepsilon_3 = 1.78\varepsilon_o$, $\varepsilon_4 = (42.5 - j0.88/\omega)\varepsilon_o$ (i.e., phantom brain tissue), and k_L $(\mathrm{m}^{-1}) = 50.6 - j10.7$. To assess the computational efficiency between the King-Casey approach and Iskander–Tumeh approach, Casey and Bansal's code (provided by Casey) and our code that uses no symmetry property are run on an HP-9000/705 workstation. For E_z data shown in Fig. 4, agreements between the two approaches are excellent; this is also true, although not shown here for brevity, for the corresponding E_ρ's and for the full-wave dipole case considered in [2]. For comparison, CPU times required by Casey and Bansal's program (with an 1% convergence) and our program (with $\Delta z' = 1$ mm) are 56.8 sec and (approximately) 0.15 s, respectively.

Next an asymmetrically driven IDA previously analyzed by Zhang *et al.* [4, Fig. 5] is examined. In this case, $f = 915$ MHz, $a = 0.47$ mm, $b = 0.584$ mm, $c = 0.8$ mm, $h_1 = 14.0$ cm, $h_2 = 3.5$ cm, $\varepsilon_2 \approx \varepsilon_o$, $\varepsilon_3 = 3.5\varepsilon_o$, $\varepsilon_4 = (51.0 - j1.28/\omega)\varepsilon_o$ (i.e., phantom muscle tissue), and $k_L(m-1) = 56.87 - j12.29$. In Fig. 5, the normalized SAR obtained by the present method using the symmetry property for observers located along a longitudinal line of $\rho = 5$ mm is compared to that reported by Zhang *et al.* in [4, Fig. 5]. In our case, $\Delta z' = \Delta z = 1$ mm $(M = N = 175)$ and $K_{\max} = 173$ are used. Except for the slightly lower SAR's found by the present method over the $z < 0$ region, the agreement between the two approaches is generally good; this also holds for the two other antennas studied by Zhang *et al.* (see [4, Figs. 3 and 4]). The CPU times required by the present method with and without the use of the symmetry property are 0.3 s and 2.1 s, respectively, on an HP-9000/720 workstation.

Finally, the near-field nature of the problem indicates that the field contributed by a given source segment decreases rapidly as its separation from the observer increases. It is thus necessary to sum contributions only from those source segments that are deemed close enough to the observer. In doing so, the computational accuracy and efficiency are determined by the degree of convergence desired. For instance, with an 1% convergence required of both field components

for the same example described in the previous paragraph, an additional threefold reduction in CPU time was achieved.

IV. Conclusion

The Iskander–Tumeh method of analysis has been demonstrated to yield accurate results with a much less CPU time. Use of the translational symmetry property to further improve its computational efficiency are also demonstated. Additional saving in CPU time is possible if the near-field nature of the problem is taken into account. Numerical experience suggest that $\Delta z' = 1$ mm, $\Delta z \geq 1$ mm, and a 1% field convergence rate should produce accurate SAR with adequate spatial resolution. Since only the symmetry property associated with F_R and F_θ terms are exploited, this algorithm is also applicable to nonuniformly insulated IDA's, for which one needs only replace (1) with appropriate section-dependent current distributions [7].

Acknowledgment

Dr. J. P. Casey's help in providing the computer program used to compute Casey and Bansal's data shown in Fig. 4 is greatly appreciated.

References

[1] R. W. P. King, B. S. Trembly, and J. Strobehn, "The electromagnetic field of an insulated antenna in a conducting or dielectric medium," *IEEE Trans. Microwave Theory Tech.*, vol. 31, pp. 574–583, July 1983.

[2] J. P. Casey and R. Bansal, "The near field of an insulated dipole in a dissipative dielectric medium," *IEEE Trans. Microwave Theory Tech.*, vol. 34, pp. 459–463, Apr. 1986.

[3] J. C. Camart, J. J. Fabre, B. Prevost, J. Pribetich, and M. Chive, "Coaxial antenna array for 915 MHz interstitial hyperthermia: Design and modelization-Power deposition and heating pattern-Phased array," *IEEE Trans. Microwave Theory Tech.*, vol. 40, pp. 2243–2250, Dec. 1992.

[4] Y. Zhang, N. V. Dubal, R. Takemoto-Hambleton, and W. T. Joines, "The determination of the electromagnetic field and SAR pattern of an interstitial applicator in a dissipative dielectric medium," *IEEE Trans. Microwave Theory Tech.*, vol. 36, pp. 1438–1444, Oct. 1988.

[5] Y. Zhang, W. T. Joines, and J. R. Oleson, "Microwave hyperthermia induced by a phased interstitial antenna array," *IEEE Trans. Microwave Theory Tech.*, vol. 38, pp. 217–221, Feb. 1990.

[6] K.L. Clibbon and A. McCowen, "Efficient computation of SAR distributions from interstitial microwave antenna arrays," *IEEE Trans. Microwave Theory Tech.*, vol. 42, pp. 595–600, Apr. 1994.

[7] M. F. Iskander and A. M. Tumeh, "Design optimization of interstitial antennas," *IEEE Trans. Biomed. Eng.*, vol. 36, pp. 238–246, Feb. 1989.

[8] R. F. Harrington, *Time Harmonic Electromagnetic Fields*. New York: McGraw-Hill, 1961, p. 79.

A Fast Integral Equation Technique for Shielded Planar Circuits Defined on Nonuniform Meshes

George V. Eleftheriades, Juan R. Mosig, and Marco Guglielmi

***Abstract*— In this contribution, the groundwork is laid out for the realization of efficient integral-equation/moment-method techniques, with arbitrary types of basis functions, for the computer-aided design (CAD) of geometrically complex packaged microwave and millimeter-wave integrated circuits (MMIC's). The proposed methodology is based on an accelerated evaluation of the Green's functions in a shielded rectangular cavity. Since the acceleration procedure is introduced at the Green's function level, it becomes possible to construct efficient shielded moment method techniques with arbitrary types of basis-functions. As an example, a Method of Moments (MoM) is implemented based on the mixed potential integral equation formulation with a rectangular, but nonuniform and nonfixed, mesh. The entire procedure can be extended to multilayer substrates.**

I. Introduction

In the framework of the Method of Moments (MoM) for shielded circuits, a major component of the CPU time is attributed to filling the MoM matrix due to the large number of summation terms involved [1]–[6]. To date, the most successful technique for addressing this filling problem is by using the fast Fourier transform (FFT) [2]–[4]. Unfortunately, the FFT restricts the underlying discretization to a fixed rectangular mesh with the corresponding subsection size limited to an integral multiple of the basic cell size. For these reasons, the FFT imposes restrictions to the accurate description of the geometries to be analyzed. In addition, the basic cells size, and thus the order of the FFT, are determined by the finest geometrical feature in the circuit and this cannot always be the most efficient choice.

Herein, the groundwork is laid out for the realization of *efficient* moment methods in a shielded environment with *arbitrary* types of basis functions. This becomes possible due to the introduction of a fast scheme for evaluating the Green's functions in a rectangular cavity. The technique begins by extracting the asymptotic part from the usual two-dimensional (2-D) modal summation form of the box Green's function [4], [5]. The asymptotic part depends on the frequency in a trivial manner and thus is expressed in terms of frequency-independent summations. Subsequently, these frequency-independent summations are transformed into a form that involves the exponentially decaying Bessel functions of the second kind. This enables to effectively collapse the original frequency-independent 2-D sinusoidal series into one-dimensional (1-D) ones. Because the acceleration process is applied at the Green's function level, the door opens to the realization of efficient MoM-based techniques with arbitrary types of basis functions.

As an example, a particular moment method has been implemented based on the mixed potential integral equation (MPIE) formulation and a nonuniform/nonfixed rectangular mesh [5], [8]. At the MoM level, special care is taken so that the interaction integrals involving the modified Bessel functions are carried out in an optimum way. Recently, an independent attempt was made in [6] to also accelerate

Manuscript received November 10, 1995; revised August 26, 1996.

G. V. Eleftheriades and J. R. Mosig are with the Laboratoire d' Electromagnetisme et d' Acoustique, Ecole Polytechnique Fédérale de Lausanne, Lausanne, CH-1015, Switzerland.

M. Guglielmi is with the European Space Research Technology Center, European Space Agency, 2200 AG Noordwijk, The Netherlands.

Publisher Item Identifier S 0018-9480(96)08496-7.